



LUND UNIVERSITY

An Overview of NQR Signal Detection Algorithms

Butt, Naveed; Gudmundson, Erik; Jakobsson, Andreas

Published in:
Magnetic Resonance Detection of Explosives and Illicit Materials

DOI:
[10.1007/978-94-007-7265-6-2](https://doi.org/10.1007/978-94-007-7265-6-2)

2014

[Link to publication](#)

Citation for published version (APA):
Butt, N., Gudmundson, E., & Jakobsson, A. (2014). An Overview of NQR Signal Detection Algorithms. In Magnetic Resonance Detection of Explosives and Illicit Materials (Vol. part 1, pp. 19-33). Springer. DOI: 10.1007/978-94-007-7265-6-2

General rights

Copyright and moral rights for the publications made accessible in the public portal are retained by the authors and/or other copyright owners and it is a condition of accessing publications that users recognise and abide by the legal requirements associated with these rights.

- Users may download and print one copy of any publication from the public portal for the purpose of private study or research.
- You may not further distribute the material or use it for any profit-making activity or commercial gain
- You may freely distribute the URL identifying the publication in the public portal

Take down policy

If you believe that this document breaches copyright please contact us providing details, and we will remove access to the work immediately and investigate your claim.

LUND UNIVERSITY

PO Box 117
221 00 Lund
+46 46-222 00 00



LUND UNIVERSITY

An Overview of NQR Signal Detection Algorithms

NAVEED R. BUTT, ERIK GUDMUNDSON, AND
ANDREAS JAKOBSSON

Published in: Magnetic Resonance Detection of
Explosives and Illicit Materials, NATO Science for
Peace and Security Series B: Physics and Biophysics
doi:10.1007/978-94-007-7265-6-2

Lund 2014

Mathematical Statistics
Centre for Mathematical Sciences
Lund University

An Overview of NQR Signal Detection Algorithms

Naveed R. Butt, Erik Gudmundson, and Andreas Jakobsson

Abstract Nuclear quadrupole resonance (NQR) is a solid-state radio frequency spectroscopic technique that can be used to detect the presence of quadrupolar nuclei, that are prevalent in many narcotics, drugs, and explosive materials. Similar to other modern spectroscopic techniques, such as nuclear magnetic resonance, and Raman spectroscopy, NQR also relies heavily on statistical signal processing systems for decision making and information extraction. This chapter provides an overview of the current state-of-the-art algorithms for detection, estimation, and classification of NQR signals. More specifically, the problem of NQR-based detection of illicit materials is considered in detail. Several single- and multi-sensor algorithms are reviewed that possess many features of practical importance, including (a) robustness to uncertainties in the assumed spectral amplitudes, (b) exploitation of the polymorphous nature of relevant compounds to improve detection, (c) ability to quantify mixtures, and (d) efficient estimation and cancellation of background noise and radio frequency interference.

The authors are at Mathematical Statistics, Centre for Mathematical Sciences, Lund University, Sweden, e-mail: {naveed, erikg, aj}@maths.lth.se. This work was supported in part by the European Research Council (ERC Grant Agreement n. 261670), the Swedish Research Council, and Carl Trygger's foundation.

1 Introduction

Nuclear quadrupole resonance (NQR) is a solid-state radio frequency (RF) spectroscopic technique that can be used to detect the presence of quadrupolar nuclei, for example ^{14}N , an element contained in many high explosives [1–5]. Furthermore, as quadrupolar nuclei are prevalent in many narcotics and drugs, NQR can also be used for drug detection and in pharmaceutical applications [6]. Recently, the technique has also been discussed in the area of oil drilling and geothermal heat drilling. NQR is related to both nuclear magnetic resonance (NMR) and magnetic resonance imaging (MRI), but does not require a large static magnetic field to split the energy levels of the nuclei. This makes it attractive as a non-invasive technique that can be used for detection of counterfeit medicines, land mines and unexploded ordnances, or for screening baggage for explosives and narcotics at airports. For instance, the currently commonly used counterfeit medicine detection technologies generally require varying degrees of sample pre-treatment or removal of pills from packages [7, 8]. In contrast, portable NQR-based sensors can be developed that custom officers and other agents of law enforcement can use without having to remove the medicines from their packaging. In case of explosive detection, contrary to metal detectors and, for instance, ground penetrating radar (GPR), NQR detects the explosive itself and its signature is unique; the NQR signal depends on the chemical structure of the molecule. Hence, in the case of land mine detection, NQR will detect the ^{14}N of the explosive, without suffering interference from, e.g., any fertilizer in the soil. Furthermore, metal detectors will have problems in magnetic soil and with mines containing very little metal¹, GPRs in clay or wet soils and with shallow mines. The NQR technique, on the other hand, suffers mainly from its inherently low signal-to-noise ratio (SNR), RF interference (RFI), and spurious signals such as piezoelectric and magnetoacoustic responses, see, e.g., [1, 3]. The low SNR can be remedied by repeating measurements, as NQR signals can be added coherently (indeed, an NQR detection system can clear its own false alarms). However, the time needed to guarantee accurate detection can be prohibitively long, especially for the case of the common explosive trinitrotoluen (TNT). RFI, on the other hand, can be alleviated using proper shielding, which, unfortunately, is only possible in laboratory environments and not when used in practice. Radio transmissions are extremely problematic for NQR signals if they lie at or near the expected locations of the NQR resonance frequencies. This is the case for TNT as it has its resonances in the radio AM band, often causing the AM signal to effectively mask the weak NQR signal. The remainder of this paper focuses on the recent advances on solutions to the aforementioned problems. We discuss different data acquisition techniques and summarize detector and interference cancellation algorithms.

¹ Data from the Cambodian Mine Action Centre, taken from March 1992 until October 1998, shows that for every mine found, there was more than 2200 false alarms, mainly due to scrap items in the ground.

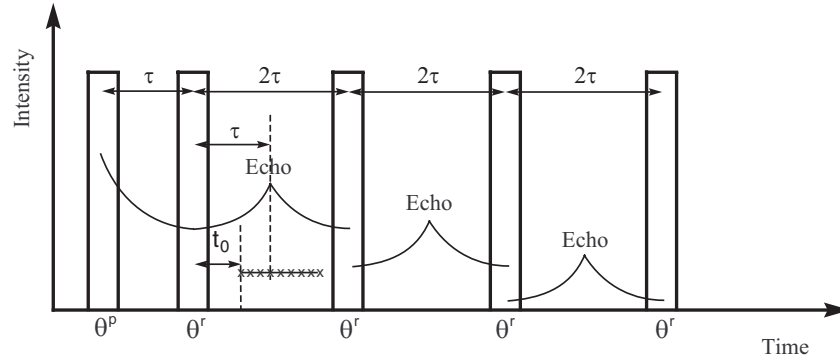


Fig. 1 Illustration of a PSL sequence.

2 Signal Models and Data Acquisition

Historically, the NQR signal has been measured as the free induction decay (FID), which is the response after a single excitation pulse. The FIDs can then be added coherently to improve the SNR, indicating that an NQR detection system is able to clear its own false alarms. However, measuring FIDs may not be the best strategy for compounds with very long spin-lattice relaxation time, T_1 , as one needs to let the system fully relax before acquiring another FID. A delay time of $5T_1$ is normally required between two excitation pulses, which could be as much as 30 seconds for substances such as TNT. To improve the SNR per time unit, several multiple pulse techniques have been proposed, of which the main techniques for detection and quantitative applications are based on steady-state free precession (SSFP) and pulsed spin locking (PSL)² sequences. An example of the former sequence is the strong off-resonant comb (SORC) [9]. Other SSFP-type sequences have been used for the detection of cocaine base [6] and the explosive RDX [10]. In the interest of brevity, we will here not further consider the SSFP techniques, merely noting that the development for PSL sequences can be paralleled for SSFP sequences. The signal obtained by PSL sequences consists of echoes that are measured between a string of pulses [1, 2], see Fig. 1. The sequence consists of a preparatory pulse, followed by a train of refocusing pulses (i.e., pulses which refocus the transverse magnetization to produce an echo), written as

$$\theta_{\angle_p}^p - (t_{sp} - \theta_{\angle_r}^r - t_{sp})_M, \quad (1)$$

where θ^p and θ^r denote the flip angles of the preparatory and refocusing pulses, respectively, while \angle_p and \angle_r denote their associated RF phases. Moreover, M is the number of refocusing pulses, or, equivalently, the number of echoes, and t_{sp}

² The PSL sequence is sometimes referred to as the spin-locking spin-echo (SLSE) sequence.

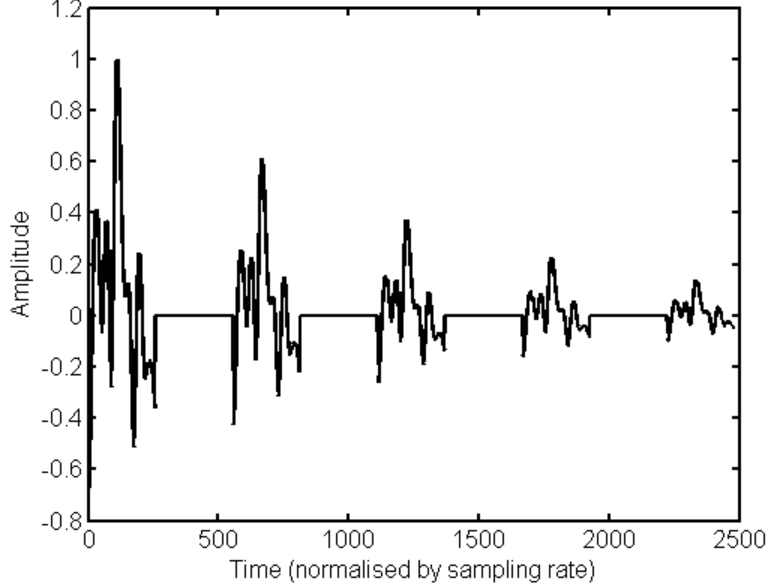


Fig. 2 Illustration of the real part of a typical echo train.

is the time (normalized with respect to the dwell time) between the center of the preparatory pulse and the center of the first refocusing pulse. This generates a train of echoes, see Fig. 2, where each individual echo can be well modeled as a sum of d exponentially damped sinusoids. In [11], the authors proposed the following model for the m th echo in the echo train:

$$y_m(t) = \sum_{k=1}^d \alpha_k e^{-\eta_k(t+m\mu)} e^{-\beta_k|t-t_{sp}|+i\omega_k(T)t} + w_m(t), \quad (2)$$

where $m = 0, \dots, M-1$ is the echo number; $t = t_0, \dots, t_{N-1}$ denotes the sampling time, measured with respect to the center of the refocusing pulse and typically starting at $t_0 \neq 0$ to allow for the deadtime between the pulse and the first measured sample; α_k , β_k , η_k , and $\omega_k(T)$ denote the complex amplitude, the sinusoidal damping constant, the echo-train damping constant, and the temperature dependent frequency shifting function of the k th sinusoid, respectively. Moreover, $w_m(t)$ denotes an additive *colored* noise, which often can be modeled using a low order autoregressive model [11, 12]. It is important to note that the number of sinusoids, d , and the frequency shifting function, $\omega_k(T)$, can generally be assumed to be known. For many compounds, such as TNT and RDX, $\omega_k(T)$ is a linear function of the temperature T at likely temperatures [13]. In Fig. 3, a periodogram spectrum of an averaged NQR signal from a shielded TNT sample is displayed. The above mentioned acquisition techniques, which we term conventional, or classical, NQR (cNQR), use powerful

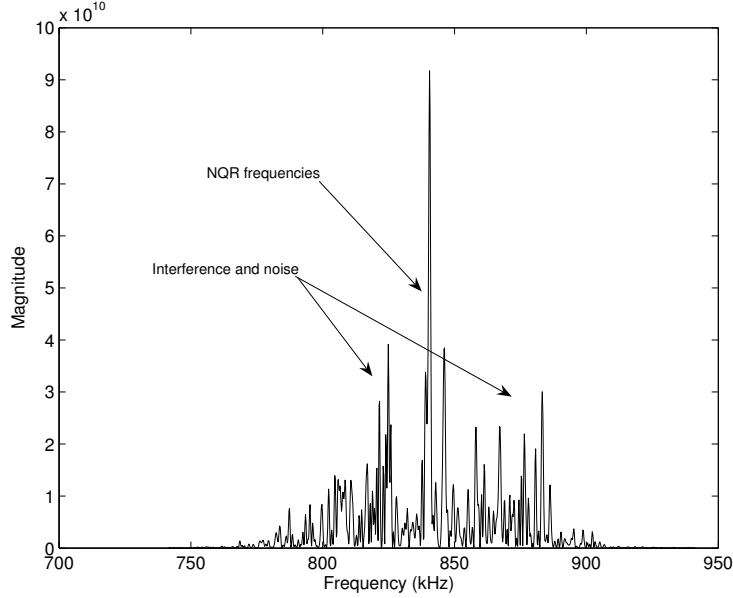


Fig. 3 Illustration of the periodogram spectrum of an NQR signal from a TNT sample.

coherent RF modulated pulses to interrogate the sample. Alternatively, one can use stochastic excitation, where the excitation sequence consists of trains of low power coherent pulses whose phases or amplitudes are randomized [14,15]. This technique is in the following termed stochastic NQR (sNQR). Provided the pulses are sufficiently weak, the sNQR system can be treated as linear and time invariant. Hence, cross-correlation of the observed time domain signal with the pseudo-white input sequence will produce an FID which can be well modeled as [15]

$$y(t) = \sum_{k=1}^d \alpha_k e^{[-\beta_k + i\omega_k(T)]t} + w(t), \quad (3)$$

where $t = t_0, \dots, t_{N-1}$. As it is not possible to acquire the signal when shooting a pulse, the FID obtained using sNQR will contain gaps and the signal will consist of blocks of regularly sampled data. Furthermore, the time between the first sample of each block is often not an integer multiple of the inter-sampling time within the blocks. In [16], the authors proposed, for NMR, to fill the gaps by repeating the measurements with different experimental settings so that the gaps occur at different times. The different signals can then be stitched together. This technique is slow and is therefore not recommended. As sNQR uses low power pulses, it has the advantage, as compared to cNQR, that it can be used to interrogate samples hidden on people and that it simplifies the construction of light-weighted, man-portable detectors for use in, e.g, land mine detection. Another advantage with sNQR is that the problem of waiting $5T_1$ between the measurements that is needed in cNQR is alle-

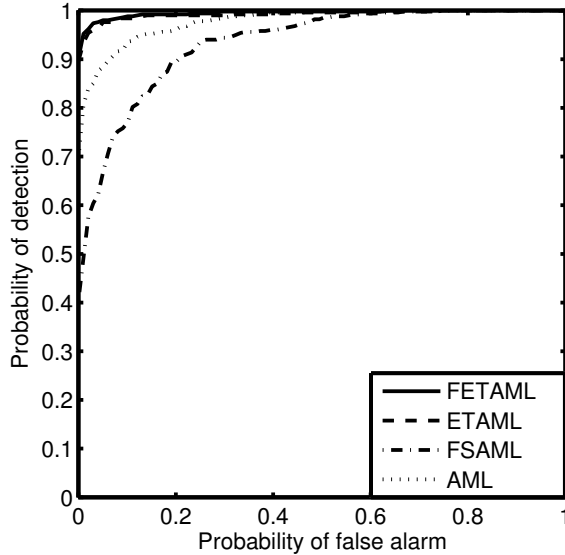


Fig. 4 ROC curves comparing state-of-the-art cNQR detectors, using partially shielded measured TNT data.

viated, and the data can, in principle, be acquired continuously. Furthermore, due to the cross-correlation, sNQR measurements are less affected by RFI and spurious signals as compared to cNQR. The advantage of cNQR over sNQR is primarily the higher SNR. Several compounds of interest appears in different crystalline structures, or polymorphs. For example, the explosive TNT exists in orthorhombic and monoclinic polymorphs, and the proportions are often not known [4]. Searching for monoclinic TNT when the explosive contains a mixture of both can severely deteriorate the detection performance [17, 18]. Sometimes the explosive is a mixture of several explosives, e.g., TNT and RDX [19]. In [17, 18], the authors proposed the following signal model for the m th echo of PSL data from a mixture of different explosives or polymorphs, or both:

$$y_m(t) = \sum_{p=1}^P \gamma_p y_m^{(p)}(t) + w_m(t), \quad (4)$$

where $y_m^{(p)}(t)$ is defined as in (2) with the addition that the model parameters depend on the p th polymorph, and where γ_p denotes the proportion of the p th polymorph. We also note that in pharmaceutical applications, it is sometimes important to know the amount of each polymorph [20, 21].

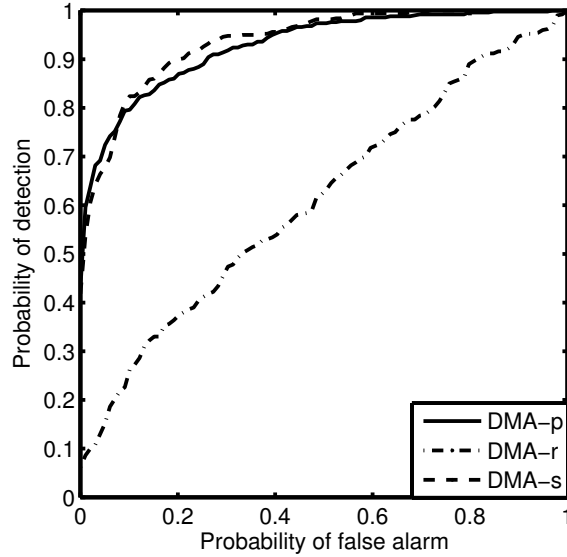


Fig. 5 ROC curves comparing state-of-the-art cNQR detectors, using partially shielded measured TNT data.

3 Detectors

During the last ten years, several NQR detectors have been proposed; however, most of them do not fully exploit the richness of the NQR model. For example, the demodulated approach (DMA) detects only one single resonance frequency. Recently, more effective detectors have been proposed, exploiting more features in the NQR model. In [22], the authors proposed using the echo train model (2) together with a matched filter; in [11, 15, 17, 23, 24], generalized likelihood ratio tests were used in combination with the models presented in Section 2. Commonly, the amplitudes of the NQR signal were considered known to a multiplicative factor; however, in practice, this would not be the case in most realistic scenarios as the field at the sample will vary, causing variations in the NQR signal amplitudes. In [25], this was remedied by allowing for uncertainties in the amplitudes, introducing the FRETAML detector. Figures 4 - 6 display the performance of some of the current state-of-the-art cNQR detectors, applied on partially shielded measured data. The FETAML and ETAML detectors are both derived using model (2), whereas FSAML and AML do not fully exploit the echo train structure. All four algorithms assume the amplitudes to be fully known, as compared to FRETAML. Furthermore, FETAML and FSAML are frequency selective. In order to utilize the possibly polymorphic structure of compounds, an extension of FETAML, termed FHETAML, was developed in [17]. FHETAML utilizes the polymorphic model in (4). In [24], FHETAML was generalized to allow for uncertainties in the assumed signal amplitudes, lead-

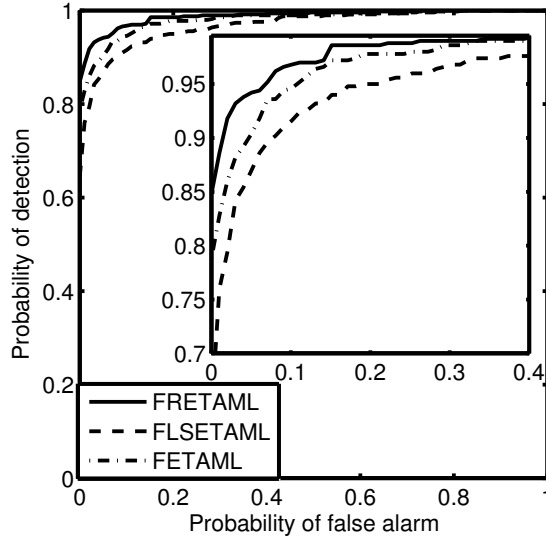


Fig. 6 ROC curves comparing state-of-the-art cNQR detectors, using partially shielded measured TNT data.

ing to the REMIQS detector. Typical comparative performance of the FHETAML and REMIQS detectors is shown in Fig. 7, where LS-FHETAML is a variant of FHETAML that does not assume any prior knowledge of the relative signal amplitudes. Common analysis and detection algorithms for echo-train data, including the ones discussed above, require some initial estimates of the expected echo decay within each echo, as well as the overall echo-train decay. Also, the number of frequency components needs to be specified. One way to retrieve initial estimates, and at the same time estimate the number of frequency components, is to use non-parametric data-adaptive estimators, such as the ones based on the Capon, APES, and IAA algorithms [?, 26]. The downside with these algorithms is that they are not able to estimate the finer structure of the echo train. To alleviate this problem, the so-called ET-CAPA algorithm was recently introduced in [27], which takes the whole echo train structure into account and estimates the damping constants for every component present in the signal. NQR measurements are often highly contaminated by powerful interference, and depending on the power and frequency of the interference, detection may be very difficult. ET-CAPA is more resilient to interference and manages to visualize both the interference and the signal of interest. This is depicted in Fig. 8 for an experimentally realistic methamphetamine NQR signal corrupted by several sinusoidal interferences. The signal of interest is located in the middle of the plot at a damping of 0.01. Even though the interference is 40 dB stronger than the signal of interest, the plot shows that the amplitudes of the interference and the signal of interest are of almost the same magnitude. This is due to the interference cancellation power of the ET-CAPA estimator, making the

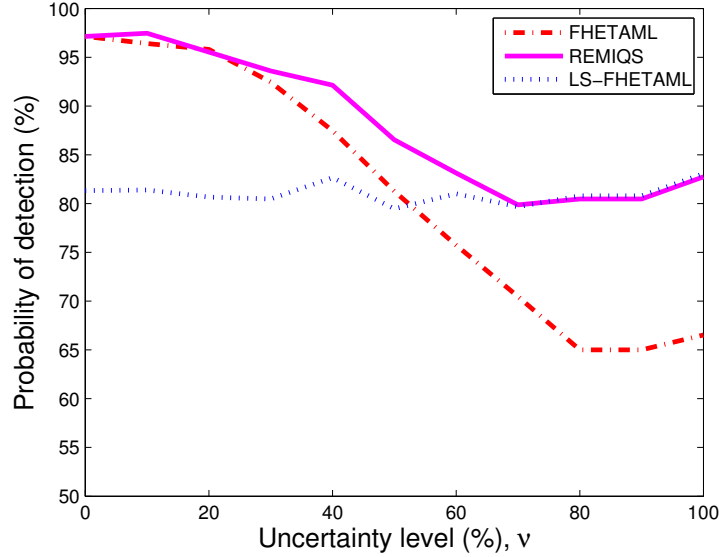


Fig. 7 Plots illustrating probability of detection as a function of the amplitude uncertainty level, v , for probability of false alarm = 2%.

signal easier to locate. The algorithm is also suitable when faced with a new or an unknown substance. In a typical NQR detection setup, one may first use ET-CAPA to get initial estimates to limit the search space, and then use previously discussed parametric methods to obtain more precise results. An alternative way to form the initial estimates of the expected echo decay and the overall echo-train decay is to use the parametric ET-ESPRIT estimator [28]. This is a computationally and statistically efficient estimator that assumes that the measured signal can be well modeled using (2), and that the additive noise may be approximated as being white, although it has been found that the estimator finds reasonably accurate estimates even in cases when these assumptions are somewhat violated. In the same work, the theoretically lower limit on the parameter's estimation variance is also presented, which may be useful in, for example, determining an appropriate SNR to achieve a desired estimation or classification accuracy. An example of how this can be done was discussed in [29], where the possible classification of different manufacturers of paracetamol was examined using such a theoretical expression. As for sNQR systems, there are notably fewer detector algorithms published and the most efficient seems to be the method published in [15]. This detector, as well as the ones shown in Figures 4-6 and Fig. 9, are CFAR, i.e., they have constant false alarm rate with respect to the power of the additive white noise. An alternative sNQR detector is also the below discussed interference-resilient REWEAL detector, which was presented in [30].

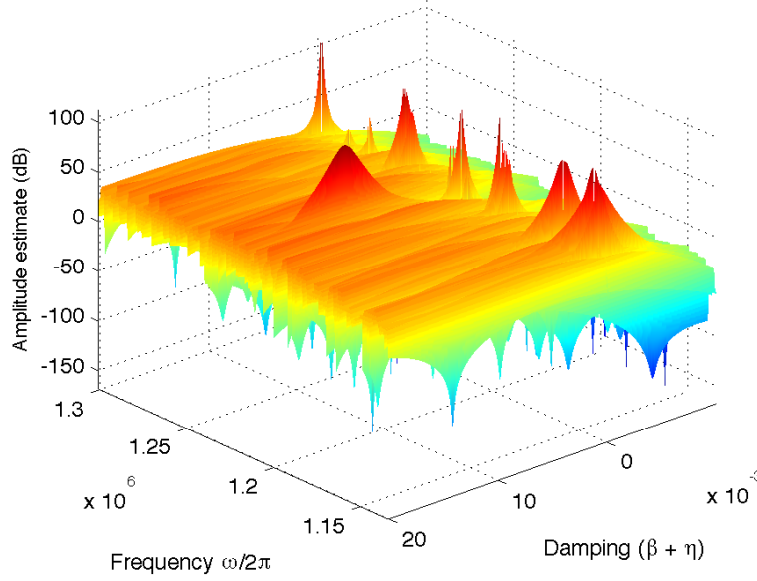


Fig. 8 The amplitude landscape for an echo-averaged experimentally realistic methamphetamine NQR signal corrupted by sinusoidal interferences.

4 Interference Rejection

One of the major concerns with NQR is the interference, both from RFI and from piezoelectric and magnetoacoustic responses caused by, e.g., sand or by metal. To remedy this, one idea is to use frequency selective algorithms, such as the one introduced in [25]. As the frequency shifting functions are known and the temperature is approximately known, the idea is to operate only on a subset of possible frequency grid points. This not only makes it possible to omit frequencies where interference signals are located, but also substantially reduces the computational complexity. In this section, we consider single-sensor detection algorithms, proceeding in the next section to also consider detectors based on spatial diversity. In [15, 31], the authors proposed highly efficient projection algorithms to remove interference signals, using the idea that secondary data, i.e., signal-of-interest (SOI) free data, can easily be acquired without additional hardware. In sNQR, only a very small amount of the data contains the FID, the rest can be considered secondary data; in cNQR, secondary data can be acquired by continuing the measurement after the pulsing has ceased. This information is used to construct an interference subspace, to which the signal is then projected orthogonally, removing the RFI components. The detectors based on these principles have shown extremely good interference cancellation properties, and simulations show that interference-to-signal ratios (ISRs) of 60 dB

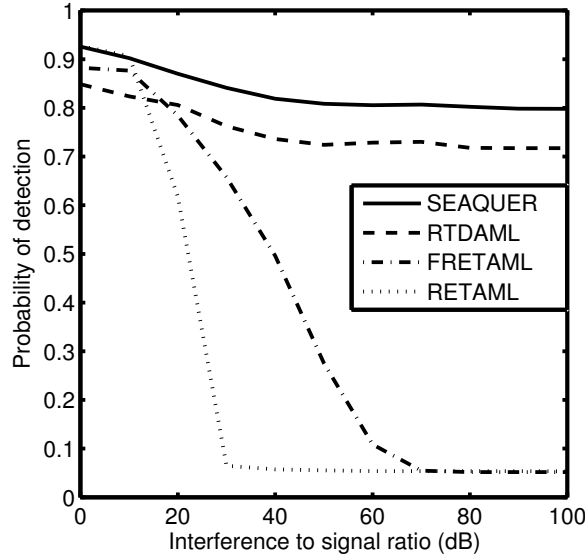


Fig. 9 Probability of detection as a function of ISR, for a probability of false alarm of 0.05, using simulated data with SNR = -28 dB.

are easily cancelled [15], without losing much detection performance; see Fig. 9, where SEAQUER denotes the projection algorithm, RTDAML is a detector where the data was prewhitened using a covariance matrix estimated from the secondary data, and RETAML is the non-frequency selective version of FRETAML. Note that the SNR is defined as the ratio of the energy of the noise-free signal and the energy of the noise. The main limitation of SEAQUER is that it does not work well when the SOI contains mixed NQR signals (e.g., from different polymorphic forms of the same substance). In order to remove this limitation, a generalization of SEAQUER, termed RESPEQ, was presented in [32]. The performance of the RESPEQ algorithm is shown in Fig. 10, where it is also compared to other state-of-the-art detection algorithms described previously. REMIQS, discussed in the previous section, takes the full polymorphic structure of the signal into account, but does not have support for dealing with the strong RFI. The suffixes (m) and (o) refer to detection of the monoclinic and the orthorhombic parts of the signal, respectively. As is seen from the figure, RESPEQ offers the best performance as it can take all polymorphs into account as well as have an effective interference rejection support. In both SEAQUER and RESPEQ, it is assumed that the SOI and the RFI reside in low dimensional signal and interference subspaces. For various reasons, such as deviations in the assumed SOI and uncertainty in the estimated interference subspace due to finite sample effects, the SOI and RFI may, however, deviate from their assumed subspaces. These errors may be in the measurements or in estimations of the subspaces, but they can alternatively be viewed as uncertainties in the subspaces.

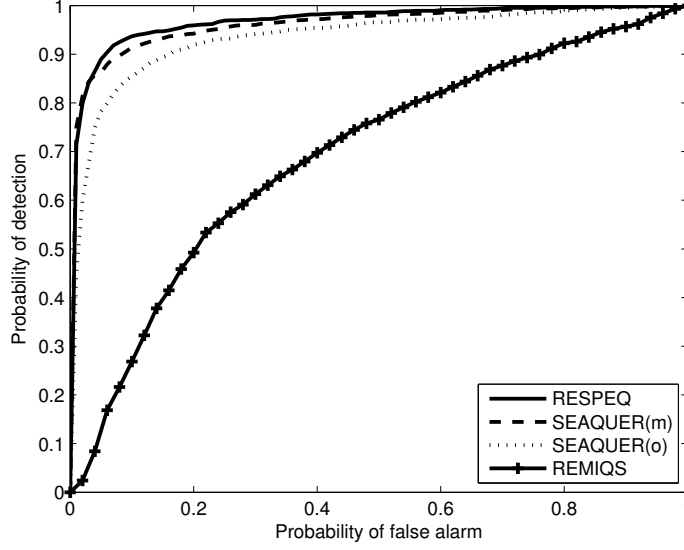


Fig. 10 ROC curves for the RESPEQ, SEAQUER, and REMIQS algorithms, for SNR = -20 dB, ISR = 40dB.

In [30], in order to compensate for these errors, the authors allowed for a small part of the energy in the signals to be outside the subspaces, leading to the REWEAL detector. REWEAL carries out interference rejection by constructing hyper-cones around the subspaces and searching for the SOI and RFI in these cones instead of in the subspaces, and is particularly useful when only small amounts of secondary data are available.

5 Multi-Channel Detectors

Using multiple antennas for efficient interference rejection in NQR-based detection has been proposed in several papers, e.g., [19, 24, 33–36], and has shown good RFI mitigation properties. Typically, one antenna is used to acquire the NQR signal and the others measure the background interference and noise. This information is then used to improve the detection. Among these, the NLS detector and the frequency-selective FSMC detector developed in [37], are based on the structured NQR signal model (2), and exploit the fact that the shifts of the spectral lines depend in a known way on temperature. In [24], FSMC is generalized to include polymorphism and to also allow for amplitude uncertainties, leading to the ESPIRE detector. Figures 11 and 12 compare the different multi-channel detectors, including the alter-

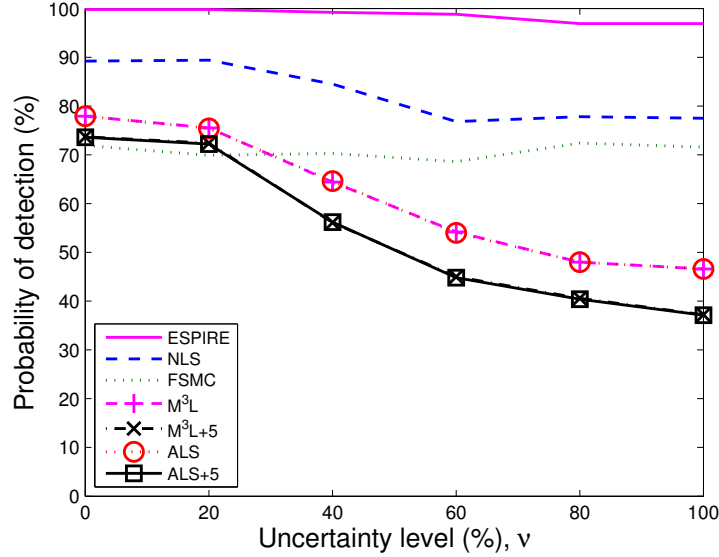


Fig. 11 Plots illustrating probability of detection as a function of the uncertainty level, v , for probability of false alarm = 8%, SNR = -36dB, with no RFI.

nating least squares (ALS) and the model-mismatched maximum likelihood (M^3L) detectors, both presented in [34], and the NLS, FSMC, and ESPIRE detectors. The NLS, FSMC and ESPIRE algorithms allow for a temperature uncertainty region of ± 10 K around the true temperature, as well as large search regions over the damping and echo damping constants. On the other hand, the ALS and M^3L detectors assume perfect knowledge of the nonlinear parameters. To mimic a more realistic scenario, however, the figures also include results for ALS and M^3L for a 5 degrees (K) offset. In a more recent work, [38] have introduced the NORRDIQ detector, that extends and improves ESPIRE by exploiting secondary data to estimate the interference subspace.

6 Concluding Remarks

In this chapter, we have discussed recent advances in the detection, classification, and identification of explosives, narcotics, and counterfeit medicines using NQR, giving an overview of the data acquisition techniques and their mathematical models. Furthermore, we have overviewed a variety of different detector and interference cancellation algorithms and compared them on both measured and simulated data.

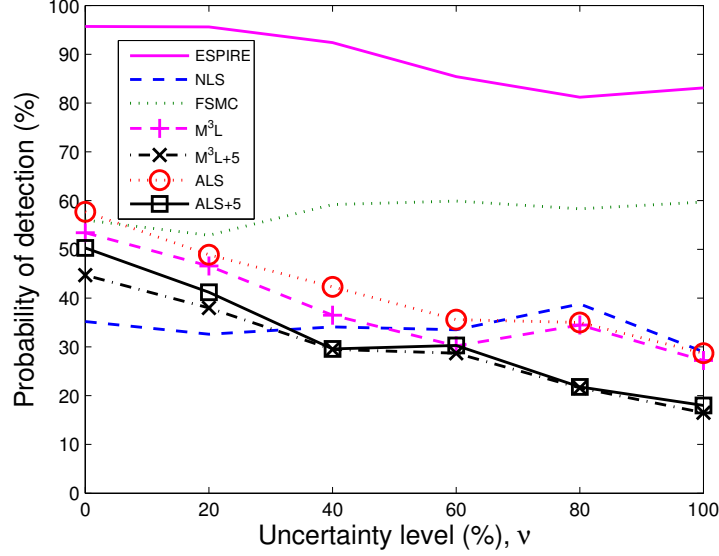


Fig. 12 Plots illustrating probability of detection as a function of the uncertainty level, v , for probability of false alarm = 8%, SNR = -36dB, ISR = 42dB.

7 Acknowledgement

The authors are grateful to their long collaboration with Prof. John Smith, Dr Jamie Barras, Dr Michael Rowe, Dr Iain Poplett, Dr Samuel Somasundaram, and Ms Georgia Kyriakidou of the NQR group at King's College London, who have been actively involved in posing and examine many of the examined problems, as well as also kindly provided all the measurements.

References

1. J. A. S. Smith, "Nitrogen-14 Quadrupole Resonance Detection of RDX and HMX Based Explosives," *European Convention on Security and Detection*, vol. 408, pp. 288–292, 1995.
2. M. D. Rowe and J. A. S. Smith, "Mine Detection by Nuclear Quadrupole Resonance," in *Proc. EUREL Int. Conf. on the Detection of Abandoned Land Mines*, Oct. 1996, pp. 62–66.
3. A. N. Garroway, M. L. Buess, J. B. Miller, B. H. Suits, A. D. Hibbs, A. G. Barrall, R. Matthews, and L. J. Burnett, "Remote Sensing by Nuclear Quadrupole Resonance," *IEEE Trans. Geosci. Remote Sens.*, vol. 39, no. 6, pp. 1108–1118, June 2001.
4. R. M. Deas, M. J. Gaskell, K. Long, N. F. Peirson, M. D. Rowe, and J. A. S. Smith, "An NQR study of the crystalline structure of TNT," in *SPIE Defense and Security Symposium*, 2004.
5. G. A. Barrall, M. Arakawa, L. S. Barabash, S. Bobroff, J. F. Chepin, K. A. Derby, A. J. Drew and K. V. Ermolaev, S. Huo, D. K. Lathrop, M. J. Steiger, S. H. Stewart, and P. J. Turner, "Advances in the Engineering of Quadrupole Resonance Landmine Detection Systems," in

- Detection and Remediation Technologies for Mines and Minelike Targets X, Proc. of SPIE*, 2005, vol. 5794.
6. J. P. Yesinowski, M. L. Buess, and A. N. Garroway, "Detection of ^{14}N and ^{35}Cl in Cocaine Base and Hydrochloride Using NQR, NMR and SQUID Techniques," *Anal. Chem.*, vol. 67, no. 13, pp. 2256–2263, July 1995.
 7. M. B. Lopes, J.-C. Wolff, J. M. Bioucas-Dias, and M. A. T. Figueiredo, "Determination of counterfeit HeptodinTM tablets by near-infrared chemical imaging and least squares estimation," *Analytica Chimica Acta*, vol. 641, pp. 46–51, 2009.
 8. C. Ricci, L. Nyadong, F. Yang, F. M. Fernandez, C. D. Brown, P. N. Newton, and S. G. Kazarian, "Assessment of hand-held Raman instrumentation for in situ screening of potentially counterfeit artesunate antimalarial tablets by FT-Raman spectroscopy and direct ionisation mass spectrometry," *Analytica Chimica Acta*, vol. 623, pp. 178–186, 2008.
 9. S. M. Klainer, T. B. Hirschfield, and R. A. Marino, "Fourier Transform NQR Spectroscopy," *Hadamard and Hilbert Transforms in Chemistry*, pp. 147–182, 1982, Editor A. G. Marshall (New York: Plenum).
 10. T. N. Rudakov and A. V. Belyakov, "Modifications of the Steady-State Free-Precession Sequence for the Detection of Pure Nuclear Quadrupole Resonance," *J. Phys. D: Appl. Phys.*, vol. 31, pp. 1251–1256, 1998.
 11. A. Jakobsson, M. Mossberg, M. Rowe, and J. A. S. Smith, "Exploiting Temperature Dependency in the Detection of NQR Signals," *IEEE Trans. Signal Process.*, vol. 54, no. 5, pp. 1610–1616, May 2006.
 12. Y. Tan, S. L. Tatum, and L. M. Collins, "Cramér-Rao Lower Bound for Estimating Quadrupole Resonance Signals in Non-Gaussian Noise," *IEEE Signal Process. Lett.*, vol. 11, no. 5, pp. 490–493, May 2004.
 13. J. A. S. Smith, M. D. Rowe, R. M. Deas, and M. J. Gaskell, "Nuclear Quadrupole Resonance Detection of Landmines," in *International Conference on Requirements and Technologies for the Detection, Removal and Neutralization of Landmines and UXO*, H. Sahli, A. M. Bottoms, and J. Cornelis, Eds., Brussels, Belgium, September 15–18 2003, vol. 2, pp. 715–721.
 14. A. N. Garroway, J. B. Miller, D. B. Zax, and M.-Y. Liao, "Method and apparatus for detecting target species having quadrupolar nuclei by stochastic nuclear quadrupole resonance," *US Patent: US5608321*, 1997.
 15. S. D. Somasundaram, A. Jakobsson, M. D. Rowe, J. A. S. Smith, N. R. Butt, and K. Althoefer, "Detecting Stochastic Nuclear Quadrupole Resonance Signals in the Presence of Strong Radio Frequency Interference," in *Proceedings of the 33rd IEEE International Conference on Acoustics, Speech and Signal Processing (ICASSP)*, Las Vegas, March 30–April 4 2008.
 16. D.-K. Yang and D. B. Zax, "Bandwidth Extension in Noise Spectroscopy," *J. Magn. Reson.*, vol. 135, pp. 267–270, 1998.
 17. S. D. Somasundaram, A. Jakobsson, and J. A. S. Smith, "Analysis of Nuclear Quadrupole Resonance Signals from Mixtures," *Signal Processing*, vol. 88, no. 1, pp. 146–157, January 2008.
 18. N. R. Butt, S. D. Somasundaram, A. Jakobsson, and J. A. S. Smith, "Frequency-Selective Robust Detection and Estimation of Polymorphic QR Signals," *Signal Processing*, vol. 88, no. 4, pp. 834–843, April 2008.
 19. H. Xiong, J. Li, and G. A. Barrall, "Joint TNT and RDX detection via quadrupole resonance," *IEEE Trans. Aerosp. Electron. Syst.*, vol. 43, no. 4, pp. 1282–1293, October 2007.
 20. E. Balchin, D. J. Malcolm-Lawes, I. J. F. Poplett, M. D. Rowe, J. A. S. Smith, G. E. S. Pearce, and S. A. C. Wren, "Potential of Nuclear Quadrupole Resonance in Pharmaceutical Analysis," *Anal. Chem.*, vol. 77, pp. 3925–3930, 2005.
 21. S. C. Pérez, L. Cerioni, A. E. Wolfenson, S. Faudone, and S. L. Cuffini, "Utilisation of Pure Nuclear Quadrupole Resonance Spectroscopy for the Study of Pharmaceutical Forms," *Int. J. Pharm.*, vol. 298, pp. 143–152, 2005.
 22. A. Gregorovič and T. Apih, "TNT detection with ^{14}N NQR: Multipulse sequences and matched filter," *J. Magn. Res.*, vol. 198, no. 2, pp. 215–221, June 2009.

23. S. D. Somasundaram, A. Jakobsson, J. A. S. Smith, and K. Althoefer, "Exploiting Spin Echo Decay in the Detection of Nuclear Quadrupole Resonance Signals," *IEEE Trans. Geosci. Remote Sens.*, vol. 45, no. 4, pp. 925–933, April 2007.
24. N. R. Butt, A. Jakobsson, S. D. Somasundaram, and J. A. S. Smith, "Robust Multichannel Detection of Mixtures Using Nuclear Quadrupole Resonance," *IEEE Trans. Signal Process.*, vol. 56, no. 10, pp. 5042–5050, October 2008.
25. S. D. Somasundaram, A. Jakobsson, and E. Gudmundson, "Robust Nuclear Quadrupole Resonance Signal Detection Allowing for Amplitude Uncertainties," *IEEE Trans. Signal Process.*, vol. 56, no. 3, pp. 887–894, March 2008.
26. E. Gudmundson, P. Stoica, J. Li, A. Jakobsson, M. D. Rowe, J. A. S. Smith, and J. Ling, "Spectral Estimation of Irregularly Sampled Exponentially Decaying Signals with Applications to RF Spectroscopy," *J. Magn. Reson.*, vol. 203, no. 1, pp. 167–176, March 2010.
27. T. Kronvall, J. Swärd, and A. Jakobsson, "Non-Parametric Data-Dependent Estimation Of Spectroscopic Echo-Train Signals," in *Proceedings of the 38th IEEE International Conference on Acoustics, Speech and Signal Processing (ICASSP)*, 2013.
28. E. Gudmundson, P. Wirfält, A. Jakobsson, and M. Jansson, "An ESPRIT-based parameter estimator for spectroscopic data," in *Proceedings of the IEEE Statistical Signal Processing Workshop (SSP'12)*, Ann Arbor, Michigan, USA, Aug. 5-8 2012.
29. H. Topa, "Detection of Counterfeit Medicines," M.S. thesis, Lund University, 2011.
30. A. Svensson and A. Jakobsson, "Adaptive Detection of a Partly Known Signal Corrupted by Strong Interference," *IEEE Signal Process. Lett.*, vol. 18, no. 12, pp. 729–732, Dec. 2011.
31. S. D. Somasundaram, A. Jakobsson, and N. R. Butt, "Countering Radio Frequency Interference in Single-Sensor Quadrupole Resonance," *IEEE Geosci. Remote Sens. Lett.*, vol. 6, no. 1, pp. 62–66, Jan. 2009.
32. T. Rudberg and A. Jakobsson, "Robust Detection of Nuclear Quadrupole Resonance Signals in a Non-Shielded Environment," in *Proceedings of the 19th European Signal Processing Conference (EUSIPCO)*, 2011.
33. Y. Tan, S. L. Tatum, and L. M. Collins, "Kalman Filtering for Enhanced Landmine Detection Using Nuclear Quadrupole Resonance," *IEEE Trans. Geosci. Remote Sens.*, vol. 43, no. 7, pp. 1507–1516, July 2005.
34. Y. Jiang, P. Stoica, and J. Li, "Array Signal Processing in the Known Waveform and Steering Vector Case," *IEEE Trans. Signal Process.*, vol. 52, no. 1, pp. 23–35, January 2004.
35. G. Liu, Y. Jiang, H. Xiong, J. Li, and G. Barrall, "Radio frequency interference suppression for landmine detection by quadrupole resonance," *EURASIP J. Applied SP*, vol. 2006, no. 29890, 2006, doi:10.1155/ASP/2006/29890.
36. P. Stoica, H. Xiong, L. Xu, and J. Li, "Adaptive beamforming for quadrupole resonance," *Digit. Signal Process.*, vol. 17, pp. 634–651, 2007.
37. A. Jakobsson and M. Mossberg, "Using Spatial Diversity to Detect Narcotics and Explosives Using NQR Signals," *IEEE Trans. Signal Process.*, vol. 55, no. 9, pp. 4721–4726, September 2007.
38. N. R. Butt and A. Jakobsson, "Efficient removal of noise and interference in multichannel quadrupole resonance," in *Proceedings of the 45th Asilomar Conference on Signals, Systems and Computers*, nov. 2011, pp. 1072–1076.